Research Article

Li Yi-hong, Niu Jin-yu, Zhao Yu-kun, He Yi-bo, Ren Zhi-feng, and Chen Hui-qin*

Study on the cladding path during the solidification process of multi-layer cladding of large steel ingots

https://doi.org/10.1515/htmp-2022-0267
received August 17, 2022; accepted December 27, 2022

Abstract: Aiming at the quality problems such as segregation, porosity and shrinkage cavities that are difficult to eliminate due to the size effect of large die-cast steel ingots as large forging blanks, the idea of layered casting of large steel ingots is proposed. The transient heat transfer process and cladding path of the ingot core and cladding layer under different molten steel casting temperatures, different ingot core diameters and different ingot core preheating temperatures were studied by combining numerical simulation and thermal experiments. The research results show that the cladding path has a certain functional relationship with the diameter of the ingot core and the preheating temperature of the ingot core. Obviously, the interfacial melting rate can be significantly improved. The thermal scaling experiment was carried out on the cladding path under the condition of a casting temperature of 1,560°C and no preheating of the ingot core. The microhardness of the interface is higher than that of the clad steel ingot, and the metallurgical bond of the interface is good.

Keywords: large steel ingot, numerical simulation, cladding path, interface bonding

1 Introduction

With the rapid development of the equipment manufacturing industry, the demand for high-quality forgings is increasing and the requirements are getting higher and higher. However, it is difficult to produce large forgings with high technical content and quality [1,2]. In large forgings, steel ingot is used as billet, and 60% of the unqualified products in production are caused by the quality problems of steel ingot. In addition, the head and tail parts of large steel ingots, which account for 40–50% of the total weight, are often removed during the billet forming process, and the material utilization rate is very low [3,4]. High-quality large steel ingot has become a bottleneck problem in the manufacture of key parts of high-end equipment.

Due to the influence of the large ingot size effect, defects such as center porosity, shrinkage cavity, segregation and inclusion usually exist in traditional multi-furnace large ingots [5,6]. The larger the ingot tonnage, the more serious the defects are, which directly leads to the deterioration of the mechanical properties of finished forgings and the decline of yield [7]. In order to overcome the above-mentioned defects, electroslag remelting technology is used in some large ingot production. But the process equipment of this method is complex. When the steel ingot is large, the cross-sectional area of the crystallizer increases, resulting in the water cooling effect of the water-cooled crystallizer on the ingot center becomes poor, the control of the sequential solidification function is weakened, the control of the center of the shrinkage cavity, and loose becomes a difficult problem [8,9]. Therefore, the quality defects of large ingot caused by the size effect cannot be eliminated even if the electroslag remelting technology is used in actual production. So, a method of multilayer coating solidification forming of large ingots was proposed. First, a solid ingot core is a cast, and then according to the size requirements of large ingot, the previously cast solid ingot core is preset in the ingot mold, and the surface of the solid ingot core is continuously wrapped. The low-temperature ingot core can absorb part of the heat of the liquid steel, improve the solidification speed and nucleation rate of the liquid steel, and refine the organization, so as to improve the internal quality of the ingot. This casting method will decompose

* **Corresponding author: Chen Hui-qin,** School of Materials Science and Engineering, Taiyuan University of Science and Technology, Taiyuan 030024, China, e-mail: S20190358@stu.tyust.edu.cn
Li Yi-hong, Niu Jin-yu, Zhao Yu-kun, He Yi-bo, Ren Zhi-feng: School of Materials Science and Engineering, Taiyuan University of Science and Technology, Taiyuan 030024, China

and refine the solidification process of large forged ingots and gradually increase the size of the ingot from small to large. The method can achieve metallurgical bonding and reduce the segregation of ingot by coating the surface of the ingot core with high-temperature molten steel.

At present, the research work on the composite forming method of steel ingot mainly includes the following: Xiong et al. [10] prepared high chromium cast iron and medium carbon steel composite ingot. The volume ratio of liquid high chromium cast iron to solid medium carbon steel during casting was 1:10, realizing metallurgical combination, and the combination surface was staggered. Liu et al. [11,12] studied the interface between high-chromium cast iron and low-carbon steel. The high chromium cast iron was placed in an argon resistance furnace and heated to 1,300°C for high-temperature coating. C Atoms diffused from the side of low carbon steel with low concentration to the side of high chromium cast iron with high concentration, effectively improving the interface bonding strength. Hou et al. [13] studied the composite interface where the roll core is Cr5 steel and the coating layer is 42CrMo steel. With the heating of electroslag, when the temperature reaches 1,600°C, part of the surface of the roll core melts to form a melting layer. At the same time, electrodes are inserted into the molten pool, the melting layer of the roll core and the coating layer are combined, and C atoms diffuse from the roll core like the coating layer with high C content. The effective metallurgical bonding between the coating layer and the roll core is ensured. However, many studies [14–17] are limited to the compound of bimetals, and the size effect is not the main influencing factor. For large ingot, Jing et al. [18,19] adopted the composite casting of the inner core billet, which fixed the ingot mold size. By changing the number of inner core billet, core preheating temperature, and core ingot diameter, they explored the influence of preheating temperature, liquid–solid ratio, and other factors on the solidification structure and interface recombination of the large ingot. The process conditions of multicore composite casting ingot were obtained to achieve the purpose of refining the solidification structure. Ren et al. [20] used a stratified pouring shape, through the metal divided into multiple packets intermittent pouring, to control the ladle from bottom to top level for solidification and achieve the purpose of effectively reducing ingot macro segregation, but the problems are different package of metal liquid cooling rate are the same, cause the solidified structure of each layer is not the same, and with the increase of ingot, each layer width increases. Solidification sequence is obvious and segregation will increase. The key to the fusion forming method is the solid bonding between metals. However, in the process of large ingot cladding, because the size of the core ingot is getting bigger and bigger, the cooling rate of cladding metal will be accelerated, resulting in limited solid–liquid metal contact time between layers, which makes it more difficult to produce metallurgical interface on the surface of core ingot cladding. At present, there is little research work in this area. Therefore, the research focus of this article is to solve metallurgical bonding between multilayer ingot when the thickness of each coating layer is what, mainly study the influence of different operating parameters on coating path and interface melting rate, to determine the solidification coating path that can achieve metallurgical bonding.

2 Materials and methods

2.1 Materials

The 30Cr2Ni4MoV steel used in the experiment has a melting point of 1,502°C, and its chemical composition is listed in Table 1. The thermal physical parameters of the steel grade, such as density, thermal conductivity and specific heat capacity, are calculated by JmatPro, and their changes with temperature are shown in Figure 1.

The material used for ingot mold is vermicular cast iron. The change of thermal conductivity and specific heat capacity with temperature is shown in Figure 2.

2.2 Methods

ANSYS Workbench software was used to simulate the transient heat transfer of the 30Cr2Ni4MoV ladle cladding process, and BRY-DZG-10 multifunctional vacuum melting and casting integrated furnace was used for thermal test verification of the cladding path, as shown in Figure 3, and its main technical parameters are shown in Table 2.

2.2.1 Simulation experiment scheme

(1) Ingot cores with diameters of 100, 150, 200, 250, 300, 350 and 400 mm and height of 3,000 mm were selected. The coating simulation was carried out for these seven ingots respectively to determine the minimum thickness that can achieve metallurgical bonding between ingots and molten steel, as shown in Table 3.

Table 1: Chemical composition of 30Cr2Ni4MoV steel

C	Si	Mn	P	S	Cr	Ni	Mo	V	Cu	Al	As	Sn	Sb	J
≤0.35	≤0.05	≤0.07	≤0.006	≤0.003	1.50–2.00	3.25–3.75	0.25–0.60	0.07–0.15	≤0.10	≤0.008	≤0.010	≤0.010	≤0.0015	≤10

Remark : J = (Si + Mn)(P + Sn) × 10^4.

(2) The ratio of liquid to solid was set as 8:1 to determine the initial coating thickness of coated ingot [18]; according to the literature, when the liquid–solid ratio is 8:1, the interface of the ingot presents a good metallurgical bond, so the liquid–solid ratio is set at 8:1 to determine the initial coating thickness of the coated ingot. Then, the coating thickness was increased or decreased according to the simulation results. Then, the calculation was re-simulated until the solid–liquid interface achieves a good metallurgical combination. The minimum change in coating thickness is 10 mm each time.
(3) When the core interface temperature reaches above the solid phase line temperature (1,437°C), it is regarded as metallurgical bonding. In the direction of height, in view of the general head and tail cutting rate of large ingot forming process is 45–50%, in order to improve the metal utilization rate, the length of the ingot core interface to achieve metallurgical bonding is more than 70% of the total height.

According to seven ingot cores with different diameters, 8:1 was used as the initial liquid–solid ratio to determine the coating thickness of ingot cores with different diameters, and the test calculation was carried out according to this parameter. According to the results of trial calculation, if the surface temperature of the ingot core cannot reach above the solid-phase line temperature, it is considered that the solid–liquid bonding surface has not reached the metallurgical bonding, and the thickness of the coating layer should be increased appropriately, and the calculation should be redone until the metallurgical bonding surface is achieved. If the surface temperature of the ingot core has reached above the solid-phase line temperature during the trial calculation based on the initially determined coating thickness, the coating thickness should be reduced appropriately and re-calculated to determine a minimum coating thickness that can make the solid–liquid bonding interface reach metallurgical bonding.

2.2.2 Establishment of geometric model and meshing

The three-dimensional (3D) model of the coated ingot was established by ANSYS Workbench sub-plate 3D modeling software Design Modeler. The model was meshed using the tetrahedral mesh, and the mesh of the contact interface between molten steel and spindle die and the contact interface between molten steel and spindle core was encrypted. Ingot mold wall thickness is designed

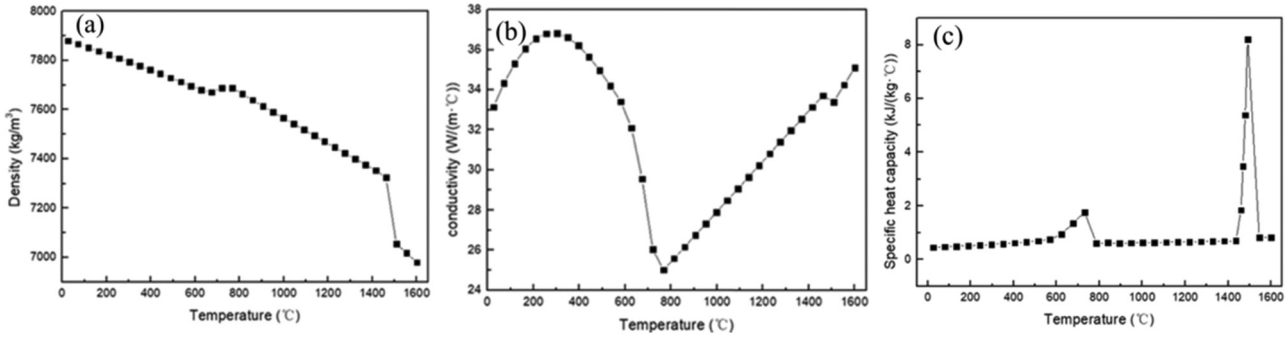

Figure 1: Variation of thermophysical parameters of 30Cr2Ni4MoV steel with temperature: (a) density; (b) thermal conductivity; (c) specific heat capacity.

according to empirical formula (1). Figure 4(a) shows the model of ingot and ingot mold with 350 mm ingot core diameter and 600 mm molten steel coating thickness.

$$Y = 113.1X + 86.5, \tag{1}$$

where Y is the thickness of the ingot mold (mm) and X is the cross-sectional area of the steel ingot (m^2).

The location of temperature measuring points was selected as shown in Figure 4(b). A temperature measuring point was taken every 500 mm along the interface height direction to observe the change of interface temperature with solidification time. Line AB is a temperature measurement line along the interface height direction. When the interface temperature reaches the maximum, the change of the interface temperature with its height at that moment. Line1, Line2 and Line3 are three temperature-measuring lines through the diameter of the ingot core, with heights of 500, 1,500 and 2,500 mm respectively. The temperature distribution inside the ingot core can be obtained by observing the temperature variation of three temperature measuring lines Line1, Line2 and Line3.

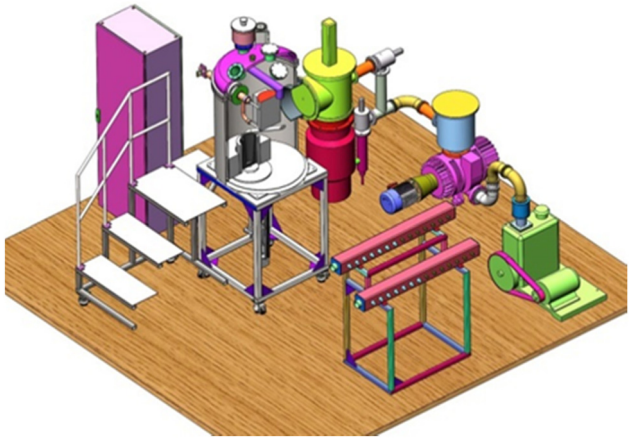

Figure 3: BRY-DZG-10 Multifunctional vacuum melting and casting furnace.

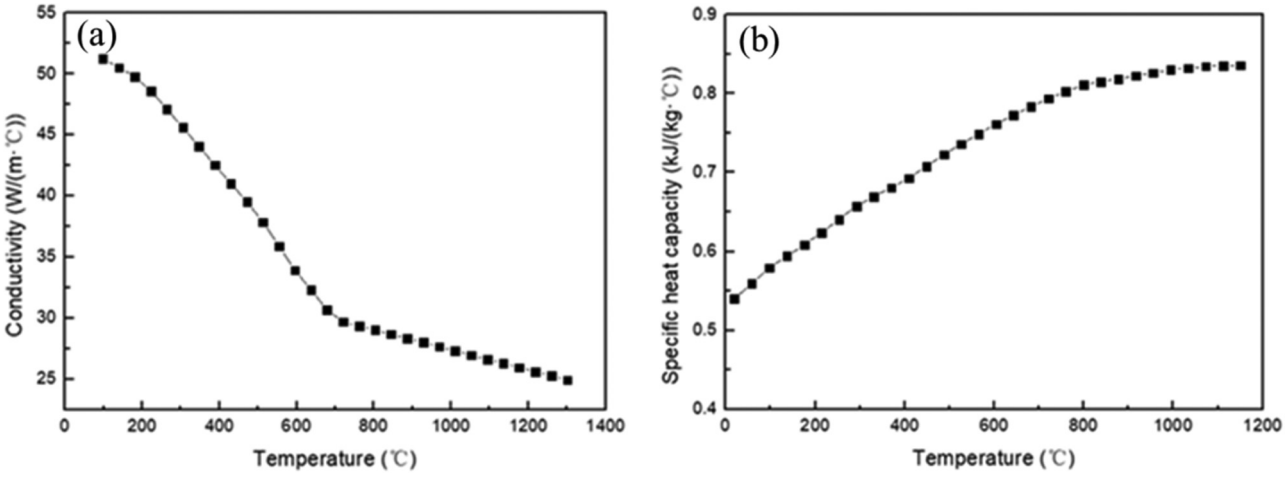

Figure 2: Variation of thermophysical parameters of compacted graphite iron with temperature: (a) thermal conductivity; (b) specific heat capacity.

Table 2: Technical parameters of BRY-DZG-10 multifunctional vacuum melting and casting furnace

Name	Unit	Parameter
Total power	kW	180
Power voltage	V	380 (three-phase supply)
Rated capacity	kg	1–10
Medium frequency rating	kW	60
Medium frequency rated frequency	kHz	2–4
Rared temperature	°C	1,700
Final vacuum (cold state of an empty stove)	Pa	6×10^{-3}

Table 3: Numerical simulation scheme

Ingot core diameter (mm)	Ingot core preheating temperature (°C)	Molten steel temperature (°C)
100, 150, 200,	No preheating	1,560
250, 300,		1,590
350, 400	400	1,560
	800	1,560

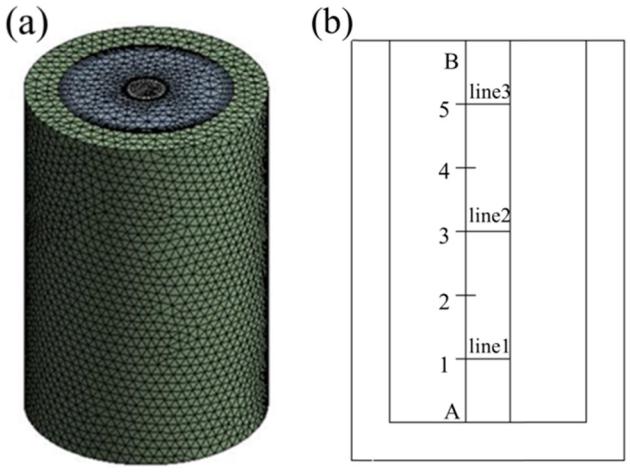

Figure 4: A steel ingot and a steel ingot mold with a core diameter of 350 mm and a molten steel coating thickness of 600 mm: (a) grid division; (b) temperature extraction position.

2.2.3 Basic assumptions

As the solidification process of steel ingot is a very complicated process, some reasonable simplification of the model is needed in the actual simulation process, and some factors that have little influence on the simulation results are ignored. In this way, the final result of the simulation can still be close to the actual result.

(1) Molten steel fills the ingot mold instantly, and the initial temperature of molten steel is the casting temperature.
(2) Without considering solute migration and undercooling, the molten steel begins to solidify when it is cooled to the liquid phase temperature [21,22].

2.2.4 Initial and boundary conditions

Initial conditions

(1) The temperature of the ingot mold is consistent with the ambient temperature, which is 27°C (300 K).
(2) The casting temperature of molten steel is 1,560°C (1,833 K).

Boundary conditions

(1) It is assumed that the molten steel surface is covered with a layer of protective slag, and the insulation surface is set between the molten steel and the protective slag.
(2) The heat transfer coefficient at the bottom of the ingot mold is set as 20 $W{\cdot}m^{-2}{\cdot}°C^{-1}$.
(3) The heat transfer coefficient between the side wall of the ingot mold and the air is set as 50 $W{\cdot}m^{-2}{\cdot}°C^{-1}$.
(4) The heat transfer coefficient between the molten steel and the ingot mold is calculated by inserting the diameter of the coated ingot into equation (2) [23].

$$h = (0.197D + 926.3) \times \left(1.832e^{-\frac{t}{73}} + 1.59e^{-\frac{t}{1,099}} + 0.09\right), \quad (2)$$

where h is the interface heat transfer coefficient ($W{\cdot}m^{-2}{\cdot}°C^{-1}$), D is the ingot diameter (mm), and t is the heat transfer time (s).

3 Analysis of experimental results

3.1 Solidification coating path of ingot core without preheating

Figure 5 shows the temperature changes with time at five temperature measuring points on the surface of the ingot core with different diameters. It can be seen from the figure that when the ingot core diameter is below 300 mm, the temperature change curves of the five temperature

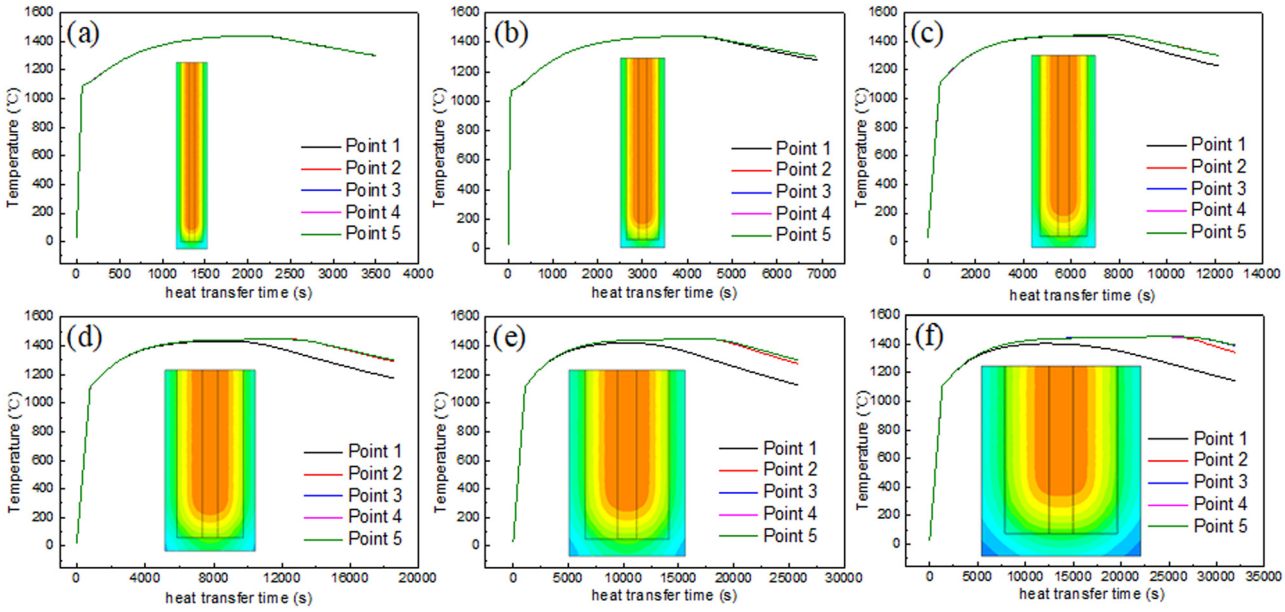

Figure 5: Variation of interfacial temperature of clad steel ingots with different diameters with time: (a) d = 150 mm; (b) d = 200 mm; (c) d = 250 mm; (d) d = 300 mm; (e) d = 350 mm; (f) d = 400 mm.

measuring points over time basically coincide. This indicates that the temperature distribution at the interface is relatively uniform. When the diameter of the ingot core exceeds 300 mm, the temperature curve of temperature measuring point 1 begins to deviate from that of the other four temperature measuring points, reaching the maximum value earlier and gradually decreasing. The temperature curve change rule of the other four points remains the same. When the diameter of the ingot core reaches more than 350 mm, the temperature measuring point 1 reaches the maximum faster than the other four temperature measuring points, and the temperature difference with the other four temperature measuring points becomes larger and larger, indicating that the temperature of the interface is no longer uniform, and the greater the diameter of the ingot core, the more serious the degree of non-uniformity. The main reasons for this phenomenon are as follows: when the diameter of the ingot core is small, the thickness of the molten steel coating layer is small, and the diameter of the coated ingot is also small. The heat emitted by the molten steel through the bottom of the ingot during solidification is limited, and most of the heat is dispersed through the side of the ingot, so the temperature distribution on the surface is uniform. With the increase of the ingot core diameter, the required coating thickness also increases, and the coated ingot diameter is twice the coating thickness plus the ingot core diameter, so the coated ingot diameter increases much faster than the ingot core diameter. As the diameter of the coated ingot increases, the heat dissipated through the bottom of the ingot increases during the solidification process. For this problem, insulation can be added to the bottom of the ingot mold to reduce heat transfer.

When the casting temperature is 1,560°C and the spindle core is not preheated, after many calculations, Figure 6 shows the changes of liquid–solid ratio and coating thickness corresponding to seven ingots with diameters of 100, 150, 200, 250, 300, 350 and 400 mm. Figure 6(a) indicates that the liquid–solid ratio increases with the diameter of the ingot core. The change of ingot coating thickness with the diameter of the ingot core is shown in Figure 6(b). It can be found that the thickness of the coating layer meets the linear relationship with the diameter of the ingot core as shown in equation (3). Through linear fitting, the obtained coating path is shown in equation (4):

$$s = k_1 d + m_1, \tag{3}$$

$$s = 1.97d - 78.57, \tag{4}$$

where s is the coating path (mm), d is the spindle core diameter(mm), k_1 is the slope, and m_1 is the intercept.

When the core diameter was 100 mm, the total diameter of the ingot was 380 mm through the first coating. At this time, 380 mm can be used as the ingot core for the second cladding. According to formula (4), it can be calculated that when the diameter of the ingot core is 380 mm, the required coating thickness is 670 mm, and the total diameter of the ingot is 1,740 mm. Because the

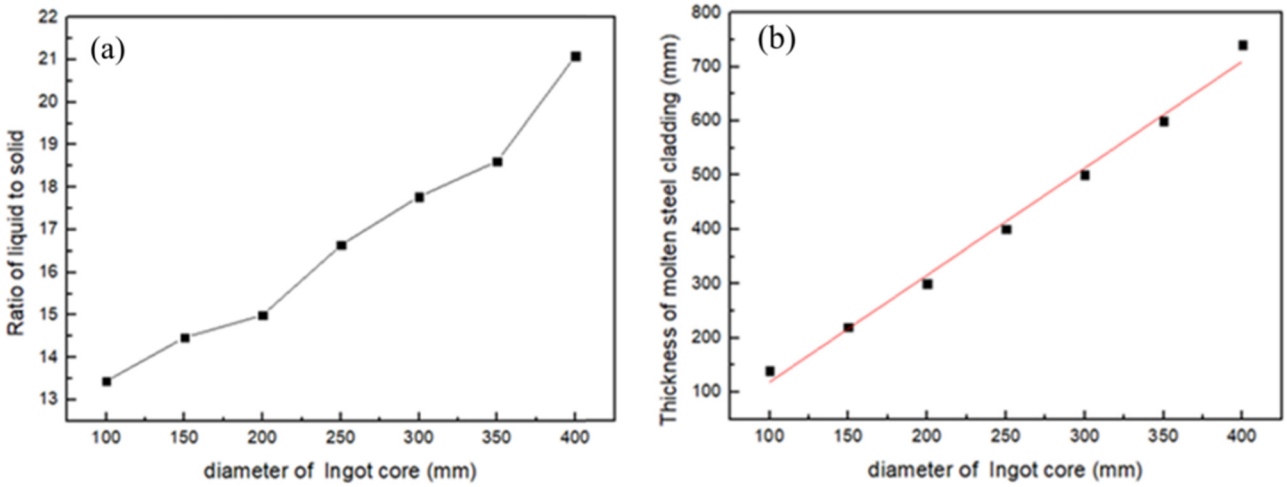

Figure 6: Variation of liquid–solid ratio and coating thickness with ingot core diameter: (a) liquid–solid ratio; (b) coating thickness.

diameter of the ingot is much larger than its height when the ingot is coated for the third time, the underside has become the main heat dissipation surface, and the molten steel dissipates too much heat through the bottom, and the ingot core interface has solidified before it can melt. Figure 7 shows the proportion of ingot core interface temperatures with different diameters that reach above the solid-phase line temperature. It can be seen from the figure that when the core diameter is 100 mm, the proportion of the interface temperature above the solid phase line is up to 93%; when the core diameter is 400 mm, the proportion of the interface temperature above the solid phase line is the lowest 72.4%. The proportion of the interface temperature above the solid phase line decreases gradually with the increase of the core diameter. Therefore, the maximum diameter of the coated ingot core is 400 mm.

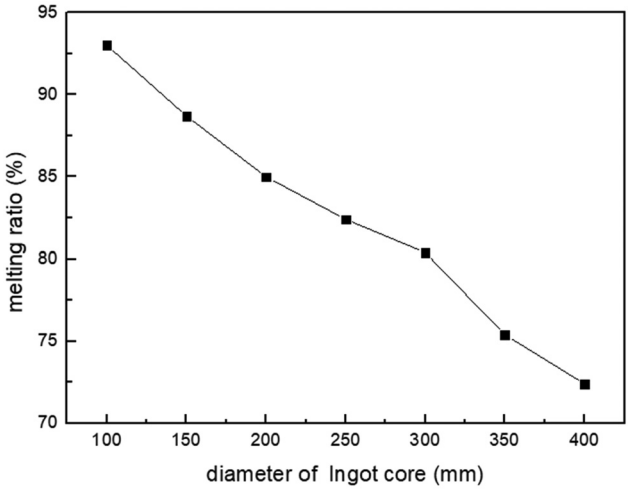

Figure 7: Interfacial melting rate between ingot core and cladding layer.

3.2 Influence of preheating temperature on coating path

Figure 8 shows the influence of different core preheating temperatures on the coating thickness when the pouring temperature of molten steel is 1,560°C. It can be seen from the figure that when the preheating temperature is 400 and 800°C, respectively, the thickness of the coating layer decreases significantly, and the larger the diameter of the spindle core is, the greater the thickness decline value of the coating layer is. When the preheating temperature is 400°C, the coating thickness of 100 mm diameter ingot decreases by 10 mm, the coating thickness of 250 mm diameter ingot decreases by 30 mm, and the coating thickness of 400 mm diameter ingot decreases by 50 mm compared with that without preheating. When the preheating temperature is 800°C, the diameter of 100 mm ingot coating thickness decreases by 20 mm than preheating at 400°C, the diameter of 250 mm ingot coating thickness decreases by 30 mm compared with preheating at 400°C, and the diameter of 400 mm ingot core decreased 80 mm compared with preheating at 400°C. The results show that the higher the preheating temperature of the ingot core is, the faster the coating thickness of the ingot decreases.

Figure 9 shows that at different preheating temperatures, the relationship between coating thickness and ingot core diameter is linear. By linear fitting, it can be obtained that the cladding paths at 400 and 800°C preheating temperature of the ingot core, respectively, satisfy equations (5) and (6):

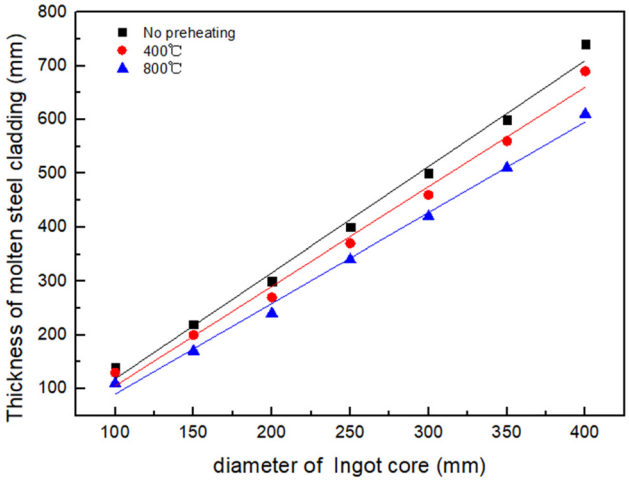

Figure 8: Thickness of the cladding layer varies with the diameter of the ingot core.

$$s_{400} = 1.85d - 79.64, \tag{5}$$

$$s_{800} = 1.68d - 78.57, \tag{6}$$

where s_{400} is the cladding path at 400°C and s_{800} is the cladding path at 800°C.

Figure 9 shows the change of coating thickness with preheating temperature under different core diameters. It can be seen from the figure that when the core diameter is fixed, the relationship between the coating thickness and the core preheating temperature meets the linear relationship shown in equation (7).

$$s = k_2T + m_2, \tag{7}$$

where T is the ingot core preheating temperature (°C), k_2 is the slope, and m_2 is the intercept.

Since the thickness of the coating layer satisfies both equations (3) and (7), the relationship between coating path, core diameter and preheating temperature must satisfy equation (8).

$$s = (k_1d + m_1) \times (k_2T + m_2). \tag{8}$$

Equation (8) is used for regression analysis of the data, and equation (9) can be obtained between coating path and ingot core diameter and preheating temperature:

$$s = -(0.062d - 2.67) \times (0.007T + 32.3). \tag{9}$$

Figure 10 shows the melting rate of the interface between ingot core and cladding layer in coated ingot with different diameters when the ingot core is not preheated and the ingot core is preheated at 400 and 800°C. The results show that the diameter of the coated ingot is 380 mm, and the melting rate is 93% when the ingot core is not preheated. The melting rate is 94.4% when the preheating temperature is 400°C. When the preheating temperature is 800°C, it is 95%, and the increase in interfacial melting rate is not obvious. The diameter of coated ingot reaches 1,880 mm, and the melting rate is 72.4% when the ingot core is not preheated. The melting rate is 76.8% when the preheating temperature is 400°C. When the preheating temperature is 800°C, it is 81.4%, and the interfacial melting rate increases obviously. This is because the interfacial melting rate is greatly affected by the heat dissipation at the bottom of the coated ingot. The larger the diameter of the coated ingot is, the more heat is emitted through the bottom of the ingot, and the molten steel near the bottom of the ingot mold has no time to melt the ingot core surface has solidified, so the larger the diameter of the coated ingot, the lower the

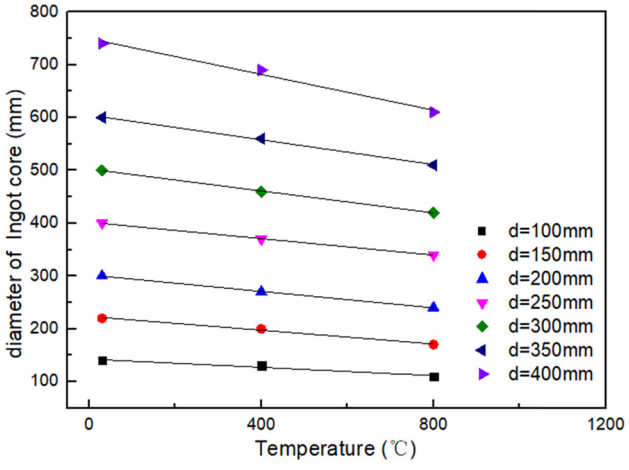

Figure 9: Variation of cladding thickness with preheating temperature.

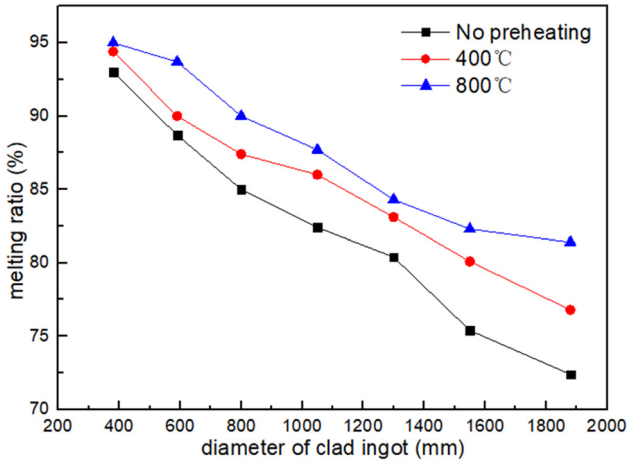

Figure 10: Surface melting rate of ingot core at different preheating temperatures.

melting rate of the interface. When the diameter of the coated ingot is small, the cooling effect of the ingot bottom is small. In addition, the coating thickness of molten steel is also small, and the solidification layer formed by molten steel during cooling and solidification process is thin, which has less hindrance to the external transmission of unsolidified heat, and the solidification and cooling speed is faster. Although the ingot core is preheated, the heat of molten steel cladding is transmitted outwardly, so the melting rate of the interface does not change much.

3.3 Effect of molten steel casting temperature on coating path

Figure 11 shows the effect of different casting temperatures on the change of coating thickness without preheating the ingot core. Considering the influence of superheat on the quality of ingot, the highest casting temperature was set at 1,590°C. It can be seen from Figure 11(a) that the change in casting temperature has little effect on the change in coating thickness. Figure 11(b) shows the effect of casting temperature on interface melting rate. It can be seen from the figure that when the casting temperature is 1,590°C compared with 1,560°C, when the ingot core diameter is over 250 mm, increasing the casting temperature can reduce the liquid–solid ratio and the growth rate of coating thickness with the ingot core diameter, but has little effect on the interface melting rate.

3.4 Analysis of hot state experimental results

3.4.1 Experimental scheme

According to the simulation results, under the condition that the ingot core is not preheated and the molten steel casting temperature is 1,560°C, the relationship between the thickness of the molten steel coating layer and the diameter of the ingot core satisfies equation (4). When the ingot core diameter is 100 mm, the coating thickness is 140 mm, and the ingot diameter is 380 mm. According to equation (4), it can be calculated that when the ingot core is 380 mm, the thickness of the molten steel coating layer is 670 mm, and the liquid–solid ratio between the molten steel and the ingot core is 19.5. In order to verify whether the molten steel and ingot core can achieve metallurgical bonding under this condition, the coated ingot of this size was scaled up. According to the size of the existing mold and the liquid–solid ratio, the size of the ingot core in the shrinkage test is 19.9 mm, and the mass of molten steel required is 7.4 kg. The experimental scheme of scale-down thermal is shown in Table 4.

3.4.2 Microstructure and element distribution of bonding interface of coated ingot

Figures 12(a) and 13(a) respectively show the metallographic structure of the solid–liquid interface at the bottom and middle of the coated ingot. It can be seen from the figure that the microstructure at the solid–liquid

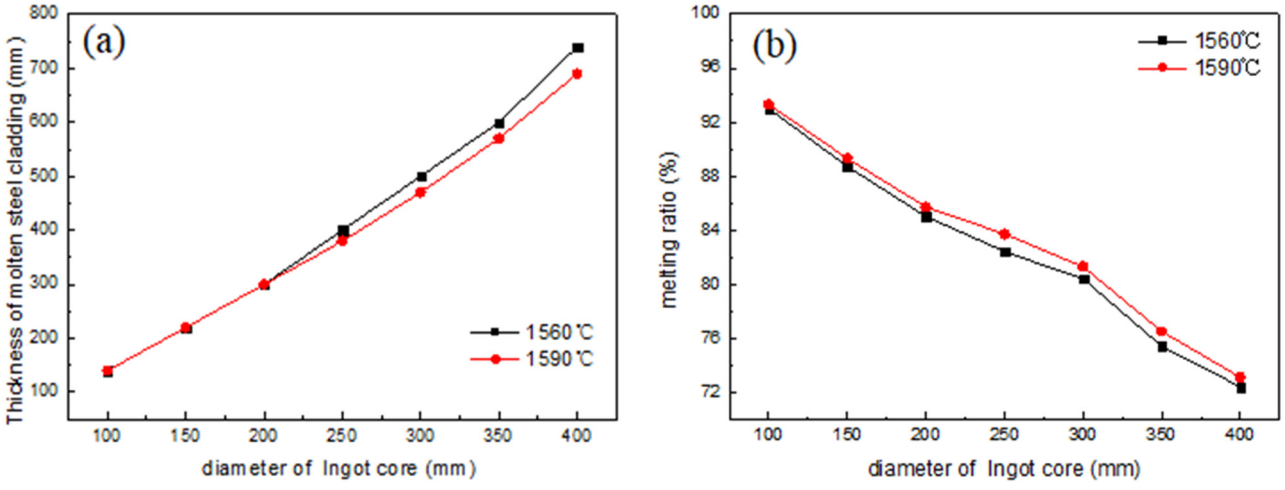

Figure 11: Effect of different casting temperatures on coated steel ingots: (a) effect of casting temperature on coating thickness; (b) effect of casting temperature on the interfacial melting rate.

Table 4: Scale-down thermal experiment scheme

Name	Unit	Parameter
Ingot core diameter	mm	19.9
Total diameter of ingot	mm	90
Molten steel temperature	°C	1,560
Molten steel quality	kg	7.4
Liquid–solid ratio	/	19.5

interface is primarily martensite and ferrite, and local ferrite is mainly arranged in parallel. The solid–liquid interface presents a jagged shape, and the bonding condition is perfect. It can be seen from Figure 12(a) that when 1,560°C molten steel is poured into the ingot mold, the temperature of molten steel in contact with the ingot core first drops and cools. Columnar crystals can be observed on the molten steel side at the solid–liquid interface. It can be seen from Figure 13(a) that when the 1,560°C molten steel is poured into the ingot mold, the heat in the middle of the ingot core is higher than that in the bottom, and the grain size at the solid–liquid interface side of the ingot core is larger, and overheating occurs at the grain boundary.

Figures 12(b) and 13(b) show the distribution of V, Cr and C elements on both sides of the bonding interface of coated steel ingot. It can be seen from the figure that the content and distribution of elements on both sides of the bonding interface between the bottom and middle of the coated ingot are consistent, indicating that the components on both sides of the solid–liquid bonding interface are the same without obvious segregation phenomenon.

3.4.3 Interfacial microhardness

A microhardness tester was used to measure the microhardness near the bonding interface. A load of 200 grams was applied for 15 seconds. The measurement results are shown in Figure 14. It can be seen from the figure that the hardness of the ingot core side is higher than that of the molten steel side, but the hardness transition of the bottom interface is gentler than that of the middle interface. At the bottom of the coated ingot, the maximum hardness is 335.6 HV and the minimum hardness is 261.3 HV. The average hardness of the ingot core side is 321 HV, and that of the molten steel side is 274 HV. The average hardness of the ingot core side is 47 HV higher than that of the molten steel side. In the middle of the coated ingot, the maximum hardness is 343.8 HV and the minimum hardness is 263.9 HV. The average hardness of the ingot core side is 332 HV, and that of the molten steel side is 280 HV. The average hardness of the ingot core side is 52 HV higher than that of the molten steel side, which is close to the hardness difference between the two sides of the bottom interface. The reason for this phenomenon is that the microstructure density of molten steel during cooling and solidification is lower than that of the ingot core. The hardness of

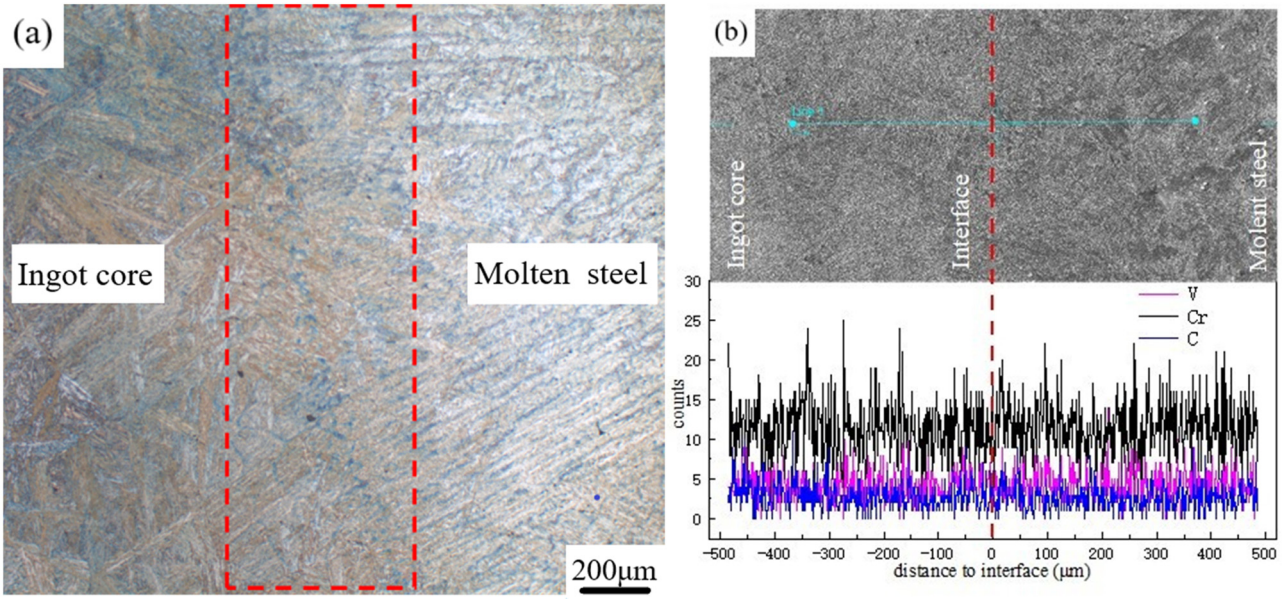

Figure 12: Metallographic structure and element distribution of solid–liquid interface at the bottom of coated steel ingot: (a) interface metallographic structure; (b) interface element distribution.

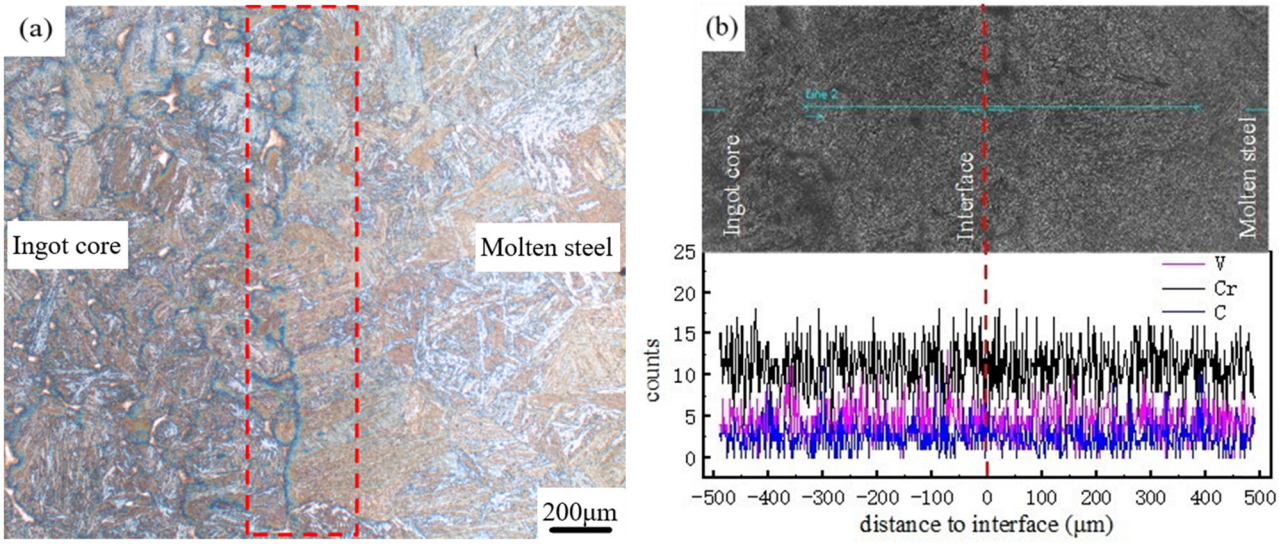

Figure 13: Metallographic structure and element distribution of solid–liquid interface in the middle of clad steel ingot: (a) interface metallographic structure; (b) interface element distribution.

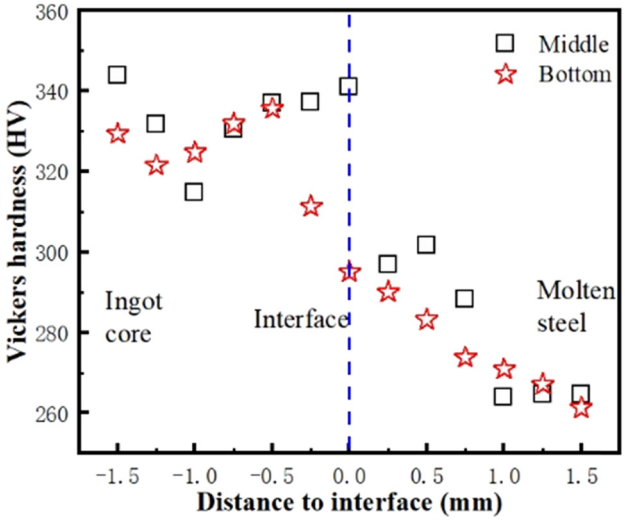

Figure 14: Microhardness near the interface.

coated ingot is lower than that of the ingot core because there is no heat treatment after the test, but the hardness of the interface is higher than that of coated ingot under the same condition without heat treatment, indicating that the interface metallurgy is well combined and the cladding path obtained by simulation is correct.

4 Conclusion

(1) When the casting temperature is 1,560°C and the ingot core is not preheated, the relationship between the thickness of the coating layer and the diameter of the ingot core meets the following requirements: $s = 1.97d - 78.57$. The coating thickness and liquid–solid ratio increase with the increase in core diameter. The solid–liquid coexistence zone on the ingot core surface widens with the increase in the diameter of the ingot core, and the melting rate on the ingot core surface decreases with the increase in the diameter of the ingot core.

(2) When the molten steel casting temperature is 1,560°C and the ingot core preheating temperature is 400°C, the coating path satisfies the formula: $s = 1.85d - 79.64$. When the core preheating temperature is 800°C, the coating path satisfies the formula: $s = 1.68d - 78.57$. The coating thickness can be significantly reduced by preheating the ingot core. In addition, the higher the preheating temperature of the core, the higher the melting rate of the core surface. The relationship between coating thickness, core diameter and preheating temperature satisfies the formula: $s = -(0.062d - 2.67) \times (0.007T + 32.3)$.

(3) When the molten steel casting temperature is 1,590°C and the ingot core diameter is more than 250 mm, increasing the casting temperature can reduce the liquid–solid ratio and the growth rate of the coating thickness with the ingot core diameter, but has little effect on the melting rate of the interface.

(4) In the hot state test, the solid–liquid interface presents a serrated shape as a whole, and the bonding condition is good. The microstructure at the interface is mainly martensite and ferrite. The results of line

scanning on both sides of the solid–liquid interface of the coated ingot show that the distribution of elements on both sides of the bottom and middle interfaces is consistent without a segregation phenomenon. The results of microhardness on both sides of the interface show that the interface hardness is higher than that of coated steel ingot, which indicates that the interface metallurgy is well combined and the cladding path of multilayer coating is correct.

Acknowledgement: The authors gratefully acknowledge financial support from the Fundamental Research Program of Shanxi Province (No. 20210302123218, No. 202103021223277), State Key Laboratory of advanced metallurgy (No. k22-10), Taiyuan University of Science and Technology Doctoral Research Fund (No. 20212025), and Research Project Supported by Shanxi Scholarship Council of China (HGKY2019084).

Funding information: This research was funded by State Key Laboratory of advanced metallurgy (No. k22-10), Fundamental Research Program of Shanxi Province (No. 20210302123218, No. 202103021223277), Taiyuan University of Science and Technology Doctoral Research Fund (No. 20212025), and Research Project Supported by Shanxi Scholarship Council of China (HGKY2019084).

Author contributions: Writing – original draft preparation, software, validation, investigation, data curation, visualization: Jinyu Niu; conceptualization, methodology, project administration, funding acquisition: Yihong Li; contribute significantly to analysis and manuscript preparation: Zhifeng Ren and Yibo He; performe the experiment: Yukun Zhao; writing – review and editing, supervision: Huiqin Chen.

Conflict of interest: The authors state no conflict of interest.

Data availability statement: All authors can confirm that all data used in this article can be published in High Temperature Materials and Processes.

References

[1] Kalyan Phani, M., S. Kanhed, S. Chakrabarti, and R. D. Patidar. Editorial Preface on the Proceedings of the 5th International Conference on Advances in Steel, Power and Construction Technology (ICASPCT 2022). *Materials Today: Proceedings*, 2022.

[2] Kim, N., D. C. Ko, N. Kang, I. Y. Oh, C. J. VanTyne, and Y. H. Moon. Feasibility of using continuously cast round bloom as a substitute to cast ingot in the manufacture of heavy forgings. *Steel Research International*, Vol. 91, 2020, id. 2000079.

[3] Park, Y. K. and J. M. Yang. Enhancing the efficiency of a die casting process using scrap recycling and ingot adjustment. *Proceedings of the Institution of Mechanical Engineers Part B Journal of Engineering Manufacture*, Vol. 225, No. 7, 2011, pp. 1105–1116.

[4] Tasan, C. C., M. Diehl, D. Yan, M. Bechtold, F. Roters, L. Schemmann, et al. An overview of dual-phase steels: Advances in microstructure-oriented processing and micromechanically guided design. *Annual Review of Materials Research*, Vol. 45, No. 1, 2015, pp. 391–431.

[5] Ling, Y., J. Zhou, H. Nan, Y. Yin, and X. Shen. A shrinkage cavity prediction model for gravity castings based on pressure distribution: A casting steel case. *Journal of Manufacturing Processes*, Vol. 26, 2017, pp. 433–445.

[6] Combeau, H., M. Založnik, S. Hans, and P. E. Richy. Prediction of macrosegregation in steel ingots: Influence of the motion and the morphology of equiaxed grains. *Metallurgical and Materials Transactions B*, Vol. 40, No. 3, 2009, pp. 289–304.

[7] Liu, X., H. Ban, J. Zhu, and B. Uy. Cyclic behaviour and modelling of stainless-clad bimetallic steels with various clad ratios. *Steel and Composite Structures, An International Journal*, Vol. 34, No. 2, 2020, pp. 189–213.

[8] Cao, Y., G. Li, Z. Jiang, Y. Dong, Z. Zhao and C. Niu. Microstructure evolution of roll core during the preparation of composite roll by electroslag remelting cladding technology. *High Temperature Materials and Processes*, Vol. 39, No. 1, 2020, pp. 270–280.

[9] Arh, B., B. Podgornik, and J. Burja. Electroslag remelting: A process overview. *Materials and Technologies*, Vol. 50, No. 6, 2016, pp. 971–979.

[10] Xiong, B., C. Cai, H. Wan, and B. Lu. Fabrication of high chromium cast iron and medium carbon steel bimetal by liquid–solid casting in electromagnetic induction field. *Materials & Design*, Vol. 32, No. 5, 2011, pp. 2978–2982.

[11] Liu, Y., Z. Zhang, G. Li, Q. Wang and B. Li. Effect of current on segregation and inclusions characteristics of dual alloy ingot processed by electroslag remelting. *High Temperature Materials and Processes*, Vol. 38, No. 2019, 2019, pp. 207–218.

[12] Li, Y., M. Gong, K. Wang, P. Li, X. Yang, and W. Tong. Diffusion behavior and mechanical properties of high chromium cast iron/low carbon steel bimetal. *Materials Science and Engineering: A*, Vol. 718, 2018, pp. 260–266.

[13] Hou, Z., Y. Dong, Z. Jiang, L. Medovar, G. Stovpchenko, T. Zou, et al. Interface bonding mechanism and heat treatment of the composite roll manufactured by electroslag remelting cladding method. *Journal of Materials Research and Technology*, Vol. 19, 2022, pp. 4115–4127.

[14] Wu, L., H. Kang, Z. Chen, Y. Fu, and T. Wang. Simulation study of Al-1Mn/Al-10Si circular clad ingots prepared by direct chill casting. *Metallurgical and Materials Transactions B*, Vol. 47, No. 1, 2016, pp. 89–98.

[15] Han, X., H. Zhang, B. Shao, L. Li, X. Liu, and J. Cui. Study on fabrication of AA4032/AA6069 cladding billet using direct chill casting process. *Journal of Materials Engineering and Performance*, Vol. 25, No. 4, 2016, pp. 1317–1326.
[16] Di Ciano, M., D. C. Weckman, and M. A. Wells. Development of an analog system to simulate interface formation during fusion™ casting. *Metallurgical and Materials Transactions B*, Vol. 47, No. 2, 2016, pp. 905–919.
[17] Caron, E. J. F. R., R. E. O. Pelayo, A. R. Baserinia, M. A. Wells, D. C. Weckman, S. Barker, et al. Direct-chill co-casting of AA3003/AA4045 aluminum ingots via fusion™ technology. *Metallurgical and Materials Transactions B*, Vol. 45, 2014, pp. 975–987.
[18] Jing, Y. A., Q. Y. Shang, P. F. Jia, X. L. Yan, Y. M. Yuan, and L. Zhang. Annealing process of cold-rolled steel strip after hydrogen reduction descaling. *Transactions of Materials and Heat Treatment*, Vol. 37, No. 4, 2016, pp. 175–182.
[19] Luo, W. D., Y. A. Jing, L. Zhang, Z. Y. Dai, M. H. Sha, and H. Song. Simulation experiment of multi-core composite casting ingot using Na_2SO_3 $5H_2O$. *Foundry Technology*, Vol. 38, No. 10, 2017, pp. 2446–2448.
[20] Ren, F., J. Wang, H. Ge, J. Li, Q. Hu, H. B. Nadendla, et al. A homogeneous billet layer casting fabrication method. *Metallurgical and Materials Transactions A*, Vol. 48, No. 10, 2017, pp. 4453–4457.
[21] Zhang, C., M. Jahazi, and R. Tremblay. Simulation and experimental validation of the effect of superheat on macro-segregation in large-size steel ingots. *The International Journal of Advanced Manufacturing Technology*, Vol. 107, No. 1, 2020, pp. 167–175.
[22] O'Mahoney, D. and D. J. Browne. Use of experiment and an inverse method to study interface heat transfer during solidification in the investment casting process. *Experimental Thermal & Fluid Science*, Vol. 22, No. 3–4, 2000, pp. 111–122.
[23] Li, Y., Y. Zhao, and H. Chen. Prediction model of interfacial heat transfer coefficient changing with time and ingot diameter. *High Temperature Materials and Processes*, Vol. 41, No. 1, 2022, pp. 238–246.